

Computational study of the rotational pathways of the amino group in 2-chloroaniline, azines and formamide: One or two rotational barriers?



Jesús Gálvez ^{a,*}, José I. López Sánchez ^{b,1}, Antonio Guirado ^b

^a Departamento de Química Física, Facultad de Química, Universidad de Murcia, Campus de Espinardo, 30071 Murcia, Apartado 4021, Spain

^b Departamento de Química Orgánica, Facultad de Química, Universidad de Murcia, Campus de Espinardo, 30071 Murcia, Apartado 4021, Spain

ARTICLE INFO

Article history:

Received 19 May 2015

Received in revised form 17 June 2015

Accepted 21 June 2015

Available online 17 July 2015

Keywords:

Amino group

Rotational pathways

Rotational barriers

ABSTRACT

Rotation of the amino group in five different molecular systems, 2-aminopyridine, 2-aminopyrimidine, 2-chloroaniline, N-methylamino-1,3,5-triazine, and formamide, has been studied at B3LYP/6-311++G(2d,2p), MP2/6-311++G(2d,2p), and CCSD(T)/6-311++G(2d,2p)//B3LYP/6-311++G(2d,2p) levels of density functional, MP2, and coupled cluster theories. To this end, detailed rotation energy profiles for the above amino systems were obtained in two different ways: (1) by computing the energy-values as a function of only one torsion angle; and (2) by taking into account that the pyramidal nature of the NH₂ group changes as rotation progresses so that energy profiles should be defined by two torsion angles. In the first case, saw-toothed energy profiles exhibiting two rotational barriers were always obtained. Conversely, by using two torsion angles as reaction coordinates smooth pathways were found where a rotation cycle can be completed passing only through the lowest energy barrier. Implications of these conflicting pathways are discussed.

© 2015 Elsevier B.V. All rights reserved.

1. Introduction

Internal rotation of the amine group is a challenging problem since it appears involved both in theoretical concepts (pyramidalization [1–3], energy barriers [1–9], molecular motors [10]) and in practical applications to biochemistry and drug design [5,8]. Most of this information could be obtained from rotation energy profiles. Unfortunately, finding the right rotational pathway is a difficult problem because complete descriptions of rotation energy profiles are not amenable to experimental study and only some specific points in the potential energy surface, namely ground state energies and rotational and inversion barriers, can be obtained. Obviously, these single points are insufficient to characterize the complete reaction pathway and so, for example, rotation energy profiles could involve more than a single transition state (TS) and, therefore, several activation energies (E_a). In most cases, however, only the highest E_a-value can be experimentally determined. Also, speculation that the presence of energy discontinuities in the rotational pathways (saw-teeth) could be associated with the

existence of unidirectional rotations and molecular motors [11,12] cannot be experimentally established. Conversely, computational methods are more suitable for such studies because they can provide detailed information on the different structures and their energies along the reaction pathway [9,13–18]. Despite these advantages, the number of computational publications including complete rotation energy profiles is rather small [2–4], especially in those cases where energy profiles need to be computed along of more than one torsion angle. Furthermore, in some cases [6] the intervals of the rotation angle at which the energies are determined are so large that significant singularities of the corresponding profiles are lost, e.g. the presence of energy discontinuities which are normally observed within a narrow interval of the torsion angle. Hence, incorrect conclusions could be drawn.

The aim of this work is to perform a detailed computational study of the rotational pathways of the amino group in five different systems, namely, 2-chloroaniline, 2-aminopyridine, 2-aminopyrimidine, N-methylamino-1,3,5-triazine, and formamide. To this end, the corresponding energy profiles have been obtained at small intervals of the torsion angles driven the rotation in two different ways: (1) by computing the energy-values as a function of only one torsion angle (this is the most common procedure which provides 2D energy profiles); and (2) by taking into account that the pyramidal nature of the NH₂ group changes as

* Corresponding author.

E-mail address: jgalvez@um.es (J. Gálvez).

¹ Present address: Dirección de Investigación, Universidad Internacional SEK Campus Miguel de Cervantes, Alberto Einstein, Carcelén, Quito, Ecuador.

rotation progresses so that rotational pathways should be defined by two torsion angles [2] leading to 3D energy profiles. In the first case, saw-toothed energy profiles exhibiting two rotational barriers in the course of a complete rotational cycle were always obtained. Conversely, by using two torsion angles as reaction coordinates, smooth pathways exist where a rotation cycle can be completed passing only through the lowest energy barrier. Implications of these conflicting pathways are discussed in next sections.

2. Computational methods

All computations have been performed with the Spartan'10 and 14 packages programs [19]. If X represent the different structures along a complete rotation cycle, i.e., $X = GS$ (ground state), ..., TS (transition state), ..., GS , and $\phi_1(X)$ and $\phi_2(X)$ are the corresponding dihedral angles defined in Fig. 1, the energy profiles were obtained as a function of one (ϕ_1) or two rotational angles (ϕ_1 and ϕ_2) given by the relationship

$$\varphi_i = \begin{cases} \phi_i(X) - \phi_i(GS), & \text{if } \phi_i(X) \geq \phi_i(GS) \\ 360^\circ + \phi_i(X) - \phi_i(GS) & \end{cases} \quad (1)$$

where $i = 1, 2$. Because all energy profiles start from the corresponding ground state full optimized structure, it follows from Eq. (1) that in the course of a complete rotational cycle $0 \leq \varphi_i \leq 360^\circ$. Rotational pathways were generated by computing energies and fully optimized structures (except by the dihedral constraints) at small intervals of φ_1 ($\approx 5^\circ$) by modifying the torsion angle $\phi_1(X)$, or varying $\phi_1(X)$ and $\phi_2(X)$ in those pathways where ϕ_1 and ϕ_2 were used as reaction coordinates. The optimization at each new geometry used the previously optimized structure as a starting point. In proximity to transitions states and near energy discontinuities in the saw-teeth, computations were performed in more detail by measuring the energy at smaller values of φ_i ($\approx 0.5^\circ$ or less). To discard that energy discontinuities were not artifacts, calculations near saw-teeth were also carried out using the very tightest tolerance for convergence. The presence of saw-teeth and energy discontinuities were not affected under these tight conditions.

Preliminary investigations of rotational pathways were performed using DFT and MP2 methods with basis sets of different

sizes (see the [Electronic Supplementary Information](#) for details). The structures obtained were then further optimized at B3LYP/6-311++G(2d,2p) and MP2/6-311++G(2d,2p) levels of theory. Both methods led to similar results and no significant differences between the results obtained with the different basis sets were found. Frequency calculations were performed at the same level of theory as the geometry optimizations to characterize the stationary points as local minima (equilibrium structures) or first-order saddle points (transition structures, TSs), as well as to obtain zero-point energy corrections (ZPE). TSs were also used to compute intrinsic reaction coordinates (IRC) at the B3LYP/6-311++G(2d,2p) level. Finally, single point energies were further refined using coupled-cluster (CC) theory at the CCSD(T)/6-311++G(2d,2p)/B3LYP/6-311++G(2d,2p) level. These improved energy-values were applied to obtain rotational barriers as the difference between the total molecular energy of the transition state (TS) and that of the ground state (GS).

3. Results and discussion

Rotation processes are frequently studied using only one torsion angle as reaction coordinate. This gives 2D energy profiles from which rotational barriers can be obtained. However, for some molecular systems the calculated rotational pathways show anomalies which are mainly due to the presence of energy discontinuities in the energy profiles. In these cases the rotation process cannot be described along only one rotation angle and it is necessary to use more than one torsion angle to calculate the corresponding pathways. For the amino systems shown in Fig. 1 a detailed study of their energy profiles has been performed at different levels of theory using both one and two torsion angles as reactions coordinates. The characteristics of the energy profiles, their energy barriers, and the pathways obtained under these conditions are illustrated in next subsections.

3.1. Calculated rotational pathways along one rotation angle

When energy profiles for the amino systems in Fig. 1 are calculated as a function of only one rotation angle they show always energy discontinuities which appear in the form of one or two saw-teeth:

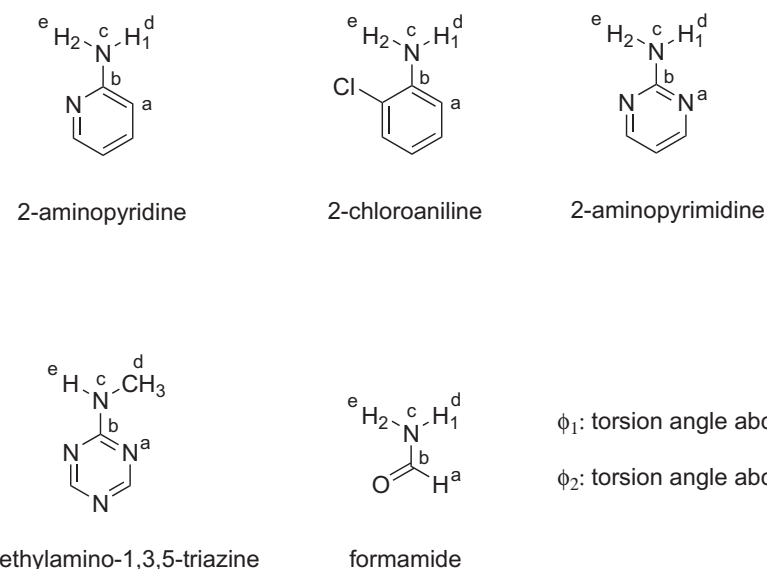


Fig. 1. Torsion angles ϕ_1 and ϕ_2 for 2-aminopyridine, 2-chloroaniline, 2-aminopyrimidine, N-methylamino-1,3,5-triazine, and formamide.

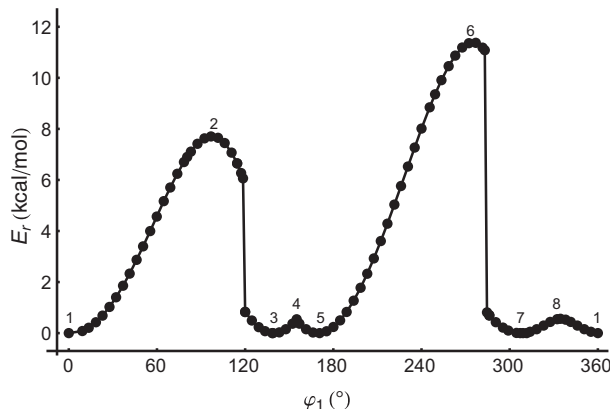


Fig. 2. Pathway for 2-aminopyridine along one rotation angle computed at the B3LYP/6-311++G(2d,2p) level: (1), (3), (5), and (7) ground state structures; (2) and (6) rotation transition states; (4) and (8) inversion transition states. Energy-values are relative to the energy of the ground state.

(A) pathway with two saw-teeth, two rotational and two inversion barriers

The energy profile of 2-aminopyridine computed at the B3LYP/6-311++G(2d,2p) level of theory as a function of the angle of rotation φ_1 is displayed in Fig. 2. This plot shows the following features: the ground state starting structure (1) ($\varphi_1 = 0^\circ$), the structure at the end of the rotation cycle ($\varphi_1 = 360^\circ$) which is identical to (1), two rotational TSs with pyramidal structures (2 and 6) whose activation energies are 7.71 and 11.39 kcal/mol, two saw-teeth following these transition states with energy discontinuities of approximately 5.2 and 10.3 kcal/mol, two planar inversion TSs (4 and 8) with the same energy barrier (0.56 kcal/mol), and three conformational isomers (3, 5, and 7) with the same energies as the ground state.

Optimized structures for the rotational and inversion transition states are shown in the [Electronic Supplementary Information](#). The lowest rotation barrier in the energy profile (7.71 kcal/mol) corresponds to the TS with the hydrogens of the amino group pointing to the nearest heteroatom of the ring (structure 2).

A schematic diagram of this kind of pathway including their representative structures is shown in Fig. 3 where transition states are displayed as dashed lines. In Fig. 3 the H₁ atom in the amino group always rotates in the same direction (counterclockwise) because φ_1 is the constraint rotational angle, while rotation of the H₂ atom is both counterclockwise (1 → 2 → 3, 5 → 6 → 7) and clockwise (3 → 4 → 5, 7 → 8 → 1). An animated sequence of the atom movements along the energy profile showing the different structures and their energies as rotation progresses is very useful as graphic support for Figs. 2 and 3, and it is provided as QuickTime movie 1 in the [Electronic Supplementary Information](#).

At DFT/B3LYP level similar pathways were also found for the other amino systems in Fig. 1, 2-aminopyrimidine, 2-chloroaniline, N-methylamino-1,3,5-triazine, and formamide, regardless of the basis set size as shown in the [Electronic Supplementary Information](#). In the case of 2-chloroaniline, energy profiles were also calculated with two alternative DFT functionals, EDF2 and w97X-D, with similar results. At MP2 level analogous pathways exhibiting two saw-teeth were obtained for 2-aminopyrimidine, N-methylamino-1,3,5-triazine, and formamide. However, for 2-aminopyridine and 2-chloroaniline the energy profiles show only one saw-tooth as described next:

(B) pathway with one saw-teeth, two rotational and one inversion barriers

Fig. 4 shows the energy profile obtained for 2-chloroaniline at the MP2/6-311++(2d,2p) level showing the following features: the ground state starting structure (1) ($\varphi_1 = 0^\circ$), the structure at

the end of the rotational cycle ($\varphi_1 = 360^\circ$) which is identical to (1), two rotational transition states with pyramidal structures (2 y 4) whose activation energies are 4.90 and 7.58 kcal/mol, one saw-tooth following the second transition state with an energy discontinuity of approximately 6.4 kcal/mol, one planar inversion TS (6) (energy barrier 1.29 kcal/mol), and two conformational isomers (3 and 5) with the same energies as the ground state. As in Fig. 2, the rotational TS with lowest activation energy is that with the hydrogens of the amino group pointing to the nearest heteroatom of the ring (structure 2). A schematic diagram of the pathway in Fig. 4 illustrating the representative structures is shown in Fig. 5 where transition states are displayed with dashed lines.² In Fig. 5 the H₁ atom in the amino group always rotates counterclockwise, while rotation of the H₂ is both counterclockwise (1 → 2 → 3 → 4 → 5) and clockwise (5 → 6 → 1). The atom movements, the corresponding structures and their energies for this pathway are illustrated in more detail in QuickTime movie 2 in the [Electronic Supplementary Information](#).

As regards rotational barriers, energy profiles along one torsion angle show for all amino systems in Fig. 1 two transition states with different energies, excepting 2-aminopyrimidine and N-methylamino-1,3,5-triazine in which, due to the symmetric position of the heteroatoms in the ring, both TSs have the same energy. In addition, inversion barriers are always present following energy discontinuities as shown in Figs. 2 and 4 and in the [Electronic Supplementary Information](#).

Finally, it should be mentioned that saw-toothed pathways (Figs. 2 and 4) calculated at large intervals of the rotation angle (specially where energy discontinuities are observed) transform into smooth profiles where inversion barriers and energy discontinuities are not longer observed. Examples are given in the [Electronic Supplementary Information](#), and they show that rotational profiles calculated with a small set of data points (or inadequate range of data) should be interpreted with caution.

3.2. Calculated rotational pathways along two rotation angles

The main difficulty with calculated rotational pathways along one rotation angle in previous section lies in the presence of saw-teeth.³ They cause that a small variation in dihedral angle φ_1 results in energy discontinuities and large changes in nuclear configuration which is not in accordance with the Born–Oppenheimer approximation. In fact, it has been suggested that energy discontinuities are caused by the impossibility of describing these kinds of pathways using only one rotation angle as reaction coordinate [12]. In particular, and regarding the rotation of the group amino, it has been considered that changes in its pyramidal character could be responsible for discontinuities in the rotation profiles so that energy profiles should be defined by using two torsion angles [2]. Hence, in next subsection rotational pathways calculated as a function of two rotation angles are discussed to address the following topics: (a) Do all computational methods provide smooth pathways without energy discontinuities? (b) Does the internal rotation of the NH₂ group necessarily pass through two rotation barriers of different energies (transition states 2 and 6 in Fig. 2, and 2 and 4 in Fig. 4)? or, (c) Conversely, does a pathway exist where a rotation cycle is completed passing only through the transition state with lowest energy

² In these schematic diagrams the horizontal line for the different amino systems is: 2-chloroaniline: C–N–C; 2-aminopyrimidine: N–N–N; N-methylamino-1,3,5-triazine: N–N–N; formamide: O–N–H. For N-methylamino-1,3,5-triazine the rotating group is HNC₂.

³ Although semiempirical methods are not appropriate for accurate studies of rotational pathways, it is worth to note that smooth energy profiles without energy discontinuities were found for some of the amino systems in Fig. 1 when PM3 and PM6 methods are used. An example is shown in the [Electronic Supplementary Information](#).

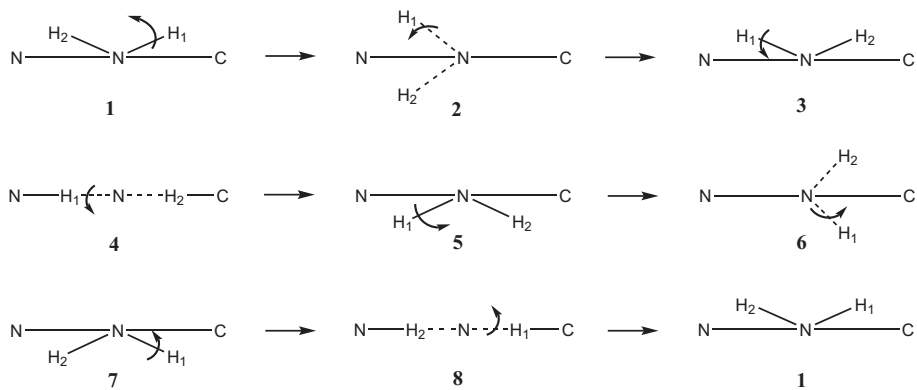


Fig. 3. Vertical top view of 2-aminopyridine. The horizontal line N-N-C represents the upper border of the ring and the atoms that are seen from the top view as located on the ring, although the nitrogen at which are attached the rotating hydrogens is not in the ring. The frames are representative structures corresponding to pathway shown in Fig. 2. Transition states (2,4,6,8) are displayed as dashed lines.

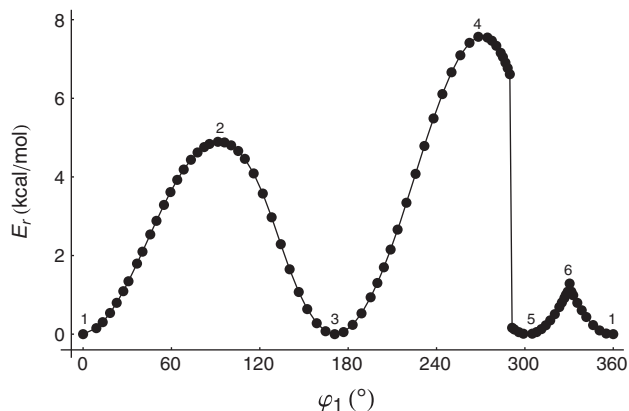


Fig. 4. Pathway for 2-chloroaniline along one rotation angle computed at the MP2/6-311++G(2d,2p) level: (1), (3), and (5) ground state structures; (2) and (4) rotation transition states; (6) inversion transition state. Energy-values are relative to the energy of the ground state.

barrier (TS 2, Figs. 2 and 4)? and (d) Is it required to pass through inversion barriers to complete a rotation cycle?

3.2.1. Smooth energy profiles with only one rotational barrier

In this section we show that if energy profiles for all amino systems given in Fig. 1 are computed as a function of the two rotational angles φ_1 and φ_2 in Eq. (1) through the dihedral angles ϕ_1 and ϕ_2 displayed in Fig. 1, smooth pathways without energy discontinuities can be obtained. In addition, these energy profiles can be chosen so that they exhibit only one rotational barrier (the one with the

lowest energy transition state) and without inversion barriers. In other words, that using φ_1 and φ_2 as reaction coordinates the saw-toothed energy profiles described in previous section can be converted into the same type of smooth pathways for all computational methods. In this type of pathway the values of energy are computed as a function of φ_1 and φ_2 and, therefore, the smooth energy profiles are 3D plots. For comparative purposes with previous 2D saw-toothed energy profiles, 2D projections of the 3D smooth pathways onto the $\varphi_1 - E_r$ and $\varphi_2 - E_r$ planes can be used.

As example, the 3D pathway of 2-aminopyridine at the B3LYP/6-311++G(2d,2p) level as a function of φ_1 and φ_2 is displayed in Fig. 6. This pathway corresponds to the saw-toothed plot in Fig. 2, and has the following features: the ground state starting structure (1) ($\varphi_i = 0^\circ$ ($i = 1, 2$)), the structure at the end of the rotation cycle ($\varphi_i = 360^\circ$ ($i = 1, 2$)) which is identical to (1), two rotation TSs with pyramidal structures (2 and 4) which now have the same activation energy (7.71 kcal/mol), and one conformational isomer (3) with the same energy as the ground state. In addition, in this type of pathway inversion barriers are not present. A schematic diagram of this pathway including the representative structures (1, 2, 3, 4, 1) is shown in Fig. 7. Also, and for comparison with the previous saw-toothed pathway obtained for this system at the same level of theory (Fig. 2), the corresponding 2D projections of the 3D energy profile in Fig. 6 onto the $\varphi_i - E_r$ ($i = 1, 2$) planes are displayed in Fig. 8.

As mentioned above, pathway in Fig. 2 have two transition states with different ring orientations and they have, therefore, different activation energies (Figs. 2 and 3). Conversely, both transition states in the 3D pathway (Fig. 6) have the same energy and orientation. Note that this orientation is always the corresponding to the lowest energy barrier, i.e. that with the two hydrogen atoms

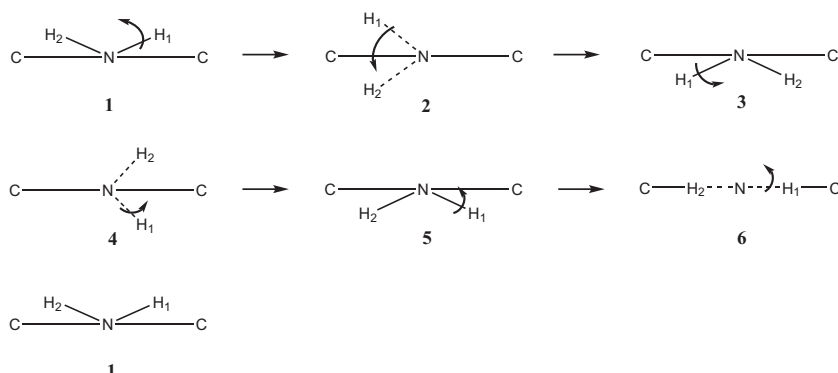


Fig. 5. Representative structures corresponding to pathway shown in Fig. 4. Transition states (2,4,6) are displayed as dashed lines. Other conditions as in Fig. 3.

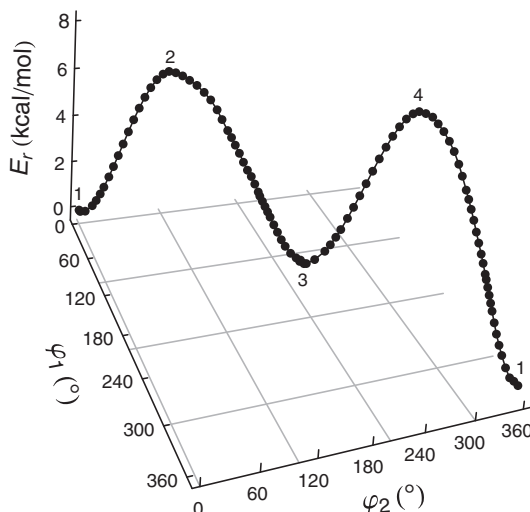


Fig. 6. 3D smooth pathway of 2-aminopyridine computed at the B3LYP/6-311++G(2d,2p) level: (1) and (3) ground state structures; (2) and (4) rotation transition states. Energy-values are relative to the energy of the ground state.

pointing to the nearest heteroatom of the ring (structures 2 and 4 in Fig. 7). Also, and unlike the rotational motion of the two hydrogen atoms in saw-toothed pathways (Figs. 2–5), the H₁ and H₂ atoms in smooth pathways always rotate counterclockwise (Figs. 6–8). QuickTime movie 3 in the [Electronic Supplementary Information](#) provides a much better visualization of the atom movements and structures along this kind of pathway.

As suggested previously, rotational pathways for the amino systems showing energy discontinuities can be transformed into 3D smooth pathways. Thus, in addition to Figs. 6 and 8 which illustrate the transformation of 2-aminopyridine saw-toothed pathway into the corresponding 3D smooth energy profile, pathway plots for the remaining amino systems in Fig. 1 computed at different levels of theory before and after being converted to 3D energy profiles are displayed in the [Electronic Supplementary Information](#).

3.2.2. Computation of smooth pathways with one rotational barrier

A rotation cycle in the 3D pathways in previous section are characterized by five reference points (1, 2, 3, 4, 1 in Figs. 6–8). Thus, and taking as example the 2-aminopyridine system (Figs. 6 and 7), in the first region of the cycle (1 → 2) the H₁ and H₂ atoms move counterclockwise toward their positions in the first transition state. In this region the rotation amplitude for the H₁ atom is larger than for the H₂, 96.40° and 71.40° respectively. In the second region (2 → 3) H₁ and H₂ continue moving counterclockwise until structure 3 is reached (conformational isomer of ground state 1). The amplitudes for H₁ and H₂ are 42.88° and 149.32°. In the third region (3 → 4) H₁ and H₂ progresses counterclockwise toward positions corresponding to the second transition state with 71.40° and 96.40° amplitudes. Finally, in the last region (4 → 1) H₁ and H₂ rotate counterclockwise to their original positions (149.32°

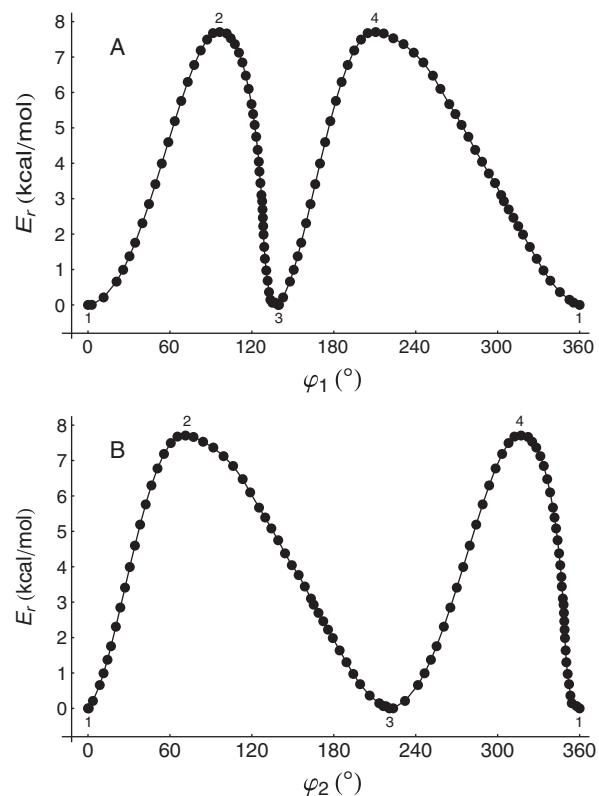


Fig. 8. Panel A: projection onto the $\varphi_1 - E_r$ plane of the 3D pathway for 2-aminopyridine displayed in Fig. 6. Panel B: As in panel A but projection is onto the $\varphi_2 - E_r$ plane. Energy-values are relative to the energy of the ground state.

and 42.88° amplitudes). Note that if we consider a rotation cycle as the result of two semicycles separated by structure 3, during the first semicycle the rotation progresses of H₁ and H₂ are 1 → 2 → 3 and 3 → 4 → 1, while during the second semicycle these rotations are 3 → 4 → 1 and 1 → 2 → 3. Hence, the rotation progress of H₁ during the first semicycle is the same as for H₂ during the second semicycle and, vice versa, the rotation progress of H₂ during the first semicycle is the same as for H₁ during the second semicycle. In this way, when rotation progresses both transition states have the structure with the lowest activation energy, and it also precludes the presence of inversion barriers during the rotation process. As far as we know, this kind of pathway has not been previously described and its behavior is completely different to that found for saw-toothed pathways in which rotation of H₁ is always forward, while rotation of H₂ shows back and forth movements (Figs. 3 and 5).

Based on these considerations the procedure adopted to compute this type of 3D pathways is as follows: (a) determination of the optimized structures corresponding to the reference points (1, 2, 3, 4, 1) (two TSs with the same activation energy (2 and 4), and two ground state structures (1 and 3)); and (b) to compute

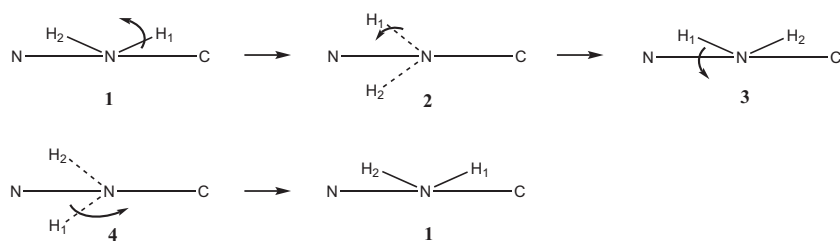


Fig. 7. Representative structures corresponding to 3D pathway shown in Figs. 6 and 7. Transition states (2,4) are displayed as dashed lines. Other conditions as in Fig. 3.

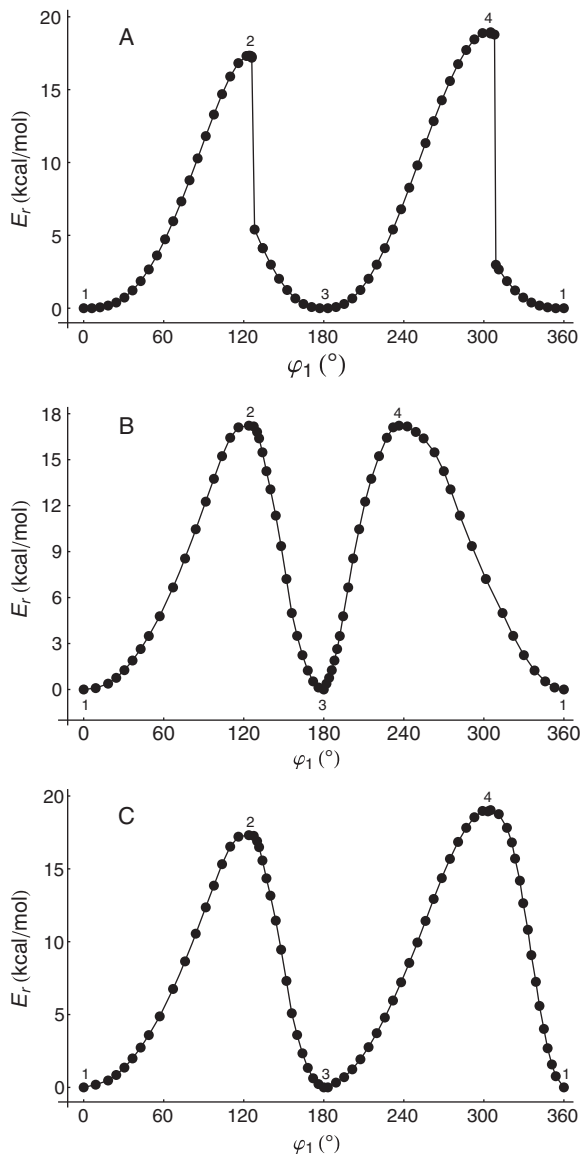


Fig. 9. Pathways for formamide computed at the MP2/6-311++G(2df,2p) level: (1) and (3) ground state structures; (2) and (4) rotation transition states. Panel A: pathway along one rotation angle. Panel B: projection onto the $\varphi_1 - E_r$ plane of the 3D smooth pathway. The two TSs have the same energy barrier and display the hydrogens of the NH₂ group pointing to the O atom. Panel C: projection onto the $\varphi_1 - E_r$ plane of a 3D smooth pathway proceeding with two TSs of different activation energies. Energy-values are relative to the energy of the ground state.

energy-values as a function of φ_i ($i = 1, 2$) in order to obtain a smooth profile connecting these points. In practice only computations for a semicycle are necessary because for the other semicycle the H₁ and H₂ atoms exchange their positions.

In any case, it is clear that because energy-values are obtained as a function of two independent variables, φ_1 and φ_2 , there are many possible pathways through which a rotation cycle can be completed. For example, smooth pathways passing through two TSs with different rotational barriers can be also generated. This is illustrated in Fig. 9 where three different energy profiles for formamide at the MP2/6-311++G(2df,2p)⁴ level have been computed for comparison. Thus, Panel A in Fig. 9 shows the saw-toothed path-

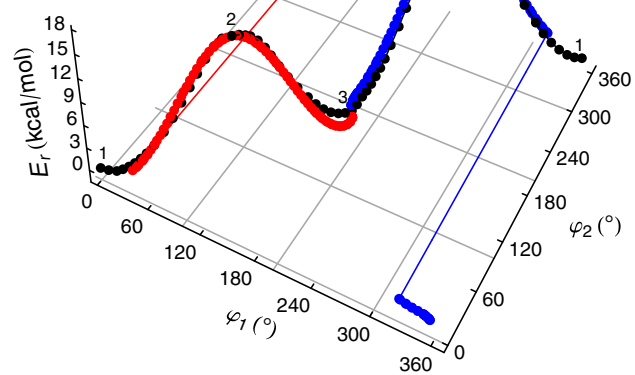


Fig. 10. 3D pathway of formamide (black), and IRC pathways from TS 2 (red) and TS 4 (blue) computed at the B3LYP/6-311++G(2d,2p) level: (1) and (3) ground state structures; (2) and (4) rotation transition states. Energy-values are relative to the energy of the ground state. IRC pathways were calculated with a stepsize = 10 (0.10 Bhor) and about 110 steps for each path. (For interpretation of the references to color in this figure legend, the reader is referred to the web version of this article.)

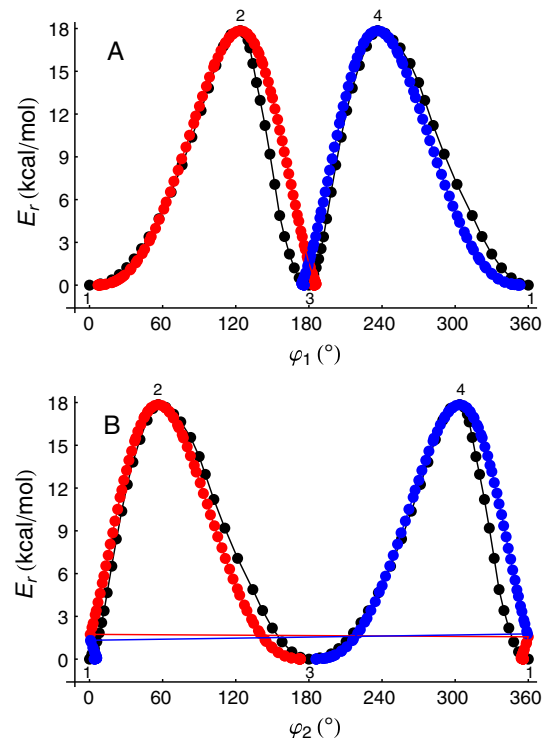


Fig. 11. Panel A: projection onto the $\varphi_1 - E_r$ plane of the 3D and IRC pathways for formamide displayed in Fig. 10. Panel B: As in panel A but projection is onto the $\varphi_2 - E_r$ plane.

way obtained when energy-values are obtained as a function of only the angle of rotation φ_1 . As discussed in previous sections, this pathway displays two TSs with different activation energies and two saw-teeth. In turn, Panel B shows the projection onto the $\varphi_2 - E_r$ plane of the 3D smooth pathway calculated as described in this section, i.e. so that the energy profile only involves the rotation barrier with the lowest activation energy. Finally, Panel C shows the projection onto the $\varphi_1 - E_r$ plane of an alternative 3D smooth energy

⁴ In this case a larger basis set was used since, as found in previous studies [20], the equilibrium geometry of the ground state of formamide at the MP2/6-311++G(2d,2p) level shows an imaginary frequency.

Table 1

Rotational barriers of the amino systems in Fig. 1.

Amino system	Theory level	$E_{a,1}(r)^a$	$E_{a,2}(r)$
2-aminopyridine	B3LYP/6-311++G(2d,2p)	7.45(7.28)	10.92(11.35)
	CCSD(T)//B3LYP/6-311++G(2d,2p)	5.71	9.25
	MP2/6-311++G(2d,2p)	5.77(5.42)	9.43(9.94)
	MP2/6-311++G(2d,2p)//B3LYP/6-311++G(2d,2p)	5.75	9.39
2-chloroaniline	B3LYP/6-311++G(2d,2p)	5.74(5.26)	8.16(8.30)
	CCSD(T)//B3LYP/6-311++G(2d,2p)	4.12	6.67
	MP2/6-311++G(2d,2p)	4.60(3.72)	7.15(6.53)
	MP2/6-311++G(2d,2p)//B3LYP/6-311++G(2d,2p)	4.53	7.13
2-aminopyrimidine	B3LYP/6-311++G(2d,2p)	13.65(13.82)	–
	CCSD(T)//B3LYP/6-311++G(2d,2p)	11.55	–
	MP2/6-311++G(2d,2p)	11.64(11.72)	–
	MP2/6-311++G(2d,2p)//B3LYP/6-311++G(2d,2p)	11.66	–
N-methylamino-1,3,5-triazine	B3LYP/6-311++G(2d,2p)	18.09(18.58)	–
	CCSD(T)//B3LYP/6-311++G(2d,2p)	15.64	–
	MP2/6-311++G(2d,2p)	16.11(16.20)	–
	MP2/6-311++G(2d,2p)//B3LYP/6-311++G(2d,2p)	15.88	–
formamide	B3LYP/6-311++G(2d,2p)	17.39(17.60)	18.69(19.43)
	CCSD(T)//B3LYP/6-311++G(2d,2p)	14.81	16.18
	MP2/6-311++G(2df,2p)	16.76(16.35)	18.24(18.77)
	MP2/6-311++G(2df,2p)//B3LYP/6-311++G(2df,2p)	16.74	18.20

^a $E_{a,i}(r)$ ($i = 1, 2$): rotational barriers in kcal/mol including ZPE corrections. For comparison values obtained with the much smaller basis set 6-31G(d) are given between parenthesis.

profile but in which rotation proceeds with two TSs of different activation energies.

As regards Fig. 9, and leaving apart the pathway exhibiting energy discontinuities (Panel A), the TSs for the pathways shown in panels B and C have been clearly determined as saddle points (they have just one imaginary frequency) with activation energies of 16.76 kcal/mol (Panel B) and 16.76 and 18.24 kcal/mol (Panel C) at the MP2/6-311++G(2df,2p) level and including ZPE corrections. It is interesting to consider which of these two pathways is more in accordance with experimental results. In this context, previous theoretical studies in the literature pointed out to pathways proceeding with two TSs of different activation energies [1,5,21], which is in agreement with the kind of pathway displays in panel C. However, and taking into account considerations based on the minimum energy pathway along the potential energy surface, the pathway involving only the lowest energy barrier should be preferred (Panel B). In fact, for the formamide only one experimental rotation barrier of 16.6 kcal/mol has been reported [22]. This is in excellent agreement with the lowest calculated value of the energy barriers and provides additional support for the smooth pathway passing only through one rotational barrier.

Anyway, discrimination between different types of pathways is a big challenge since experimentally only ground state energies and energy barriers can be determined. This precludes that a complete description of rotation pathways can be obtained and raises many questions about the characteristics of these processes that still remain to be elucidated.

4. Intrinsic reaction coordinate calculations

Intrinsic Reaction Coordinate (IRC) pathways are useful to establish the connection between the transition states and the corresponding local minima along the reaction pathways. To verify if saw-toothed or smooth energy profiles are involved with the rotational pathways of the amino group IRC calculations were performed starting from the located transition states 2 and 4 (see Fig. 6 and 7).

As example, the 3D and IRC pathways of formamide computed at the B3LYP/6-311++G(2d,2p) level of theory as a function of φ_1 and φ_2 are displayed in Fig. 10. In turn, the corresponding 2D

projections of these 3D energy pathways onto the $\varphi_i - E_r$ ($i = 1, 2$) planes are shown in Fig. 11. These figures reveal that a good agreement in the regions close to both transition states exists, although some of the IRC points near the local minima are anomalous (these anomalous points reach the ground state when submitted to a geometry optimization).

IRC computations at the B3LYP/6-311++G(2d,2p) level were also carried out for 2-aminopyridine, 2-aminopyrimidine and 2-chloroaniline. For 2-aminopyrimidine and 2-aminopyridine the results were similar to those shown in Figs. 10 and 11. However, for 2-chloroaniline the calculation process failed after a few IRC steps.

5. Rotational barriers

As discussed above, all amino systems in Fig. 1 show two transition states with different energies, excepting 2-aminopyrimidine and N-methylamino-1,3,5-triazine in which, due to the symmetric position of the heteroatoms in the ring, the two transition states have the same energy. Also, it has been shown that rotation through 3D smooth pathways takes place without inversion barriers and for this reason they are not discussed here. Regarding rotational barriers, 3D smooth pathways exist in which a rotation cycle can be completed passing only through the transition state with the lowest activation energy (Panel B in Fig. 9), although alternative 3D pathways can be also chosen so rotation takes place through both TSs (panel C in Fig. 9). The E_a -values for the two TSs of the amino systems in Fig. 1 computed at DFT, MP2 and CCSD(T) levels and including ZPE corrections calculated at the same level of theory as the geometry optimizations are summarized in Table 1.

6. Conclusions

The computational study of rotational pathways of the amino group in 2-chloroaniline, 2-aminopyridine, 2-aminopyrimidine, N-methylamino-1,3,5-triazine, and formamide, has been performed by applying DFT, MP2, and CCSD(T) methods. If energy-values are calculated using only one torsion angle energy discontinuities associated to large changes in nuclear configuration

are always obtained which seem difficult to explain in the light of the Born–Oppenheimer approximation. Conversely, when the values of energy are computed as a function of two angles of rotation, smooth profiles that are free of the above anomalies are obtained at DFT and MP2 levels including the CCSD(T)//B3LYP/6-311++G(2d,2p) energy profile for formamide which is displayed in the [Electronic Supplementary Information](#). These pathways proceed with no inversion barriers and can be chosen so that they pass only through the rotation barrier with the lowest activation energy.

Acknowledgements

We thank very much one of the reviewers for his insightful and constructive observation that should be of great interest a comparison between Intrinsic Reaction Coordinate (IRC) pathways obtained starting from the located transition states 2 and 4 (see Fig. 6 and 7) and the energy profiles computed as described in previous sections using φ_1 and φ_2 as reaction coordinates

Appendix A. Supplementary material

Computational results: (1) QuickTime movies for 2-aminopyridine and 2-chloroaniline pathways, with and without energy discontinuities, showing the atom movements and the corresponding structures and their energies as rotation progresses; (2) energy profiles for 2-aminopyridine, 2-chloroaniline, 2-aminopyrimidine, N-methylamino-1,3,5-triazine, and formamide computed at different levels of theory by using one and two rotation angles. Supplementary data associated with this article can be found, in the online version, at <http://dx.doi.org/10.1016/j.comptc.2015.06.020>. These data include MOL files and InChiKeys of the most important compounds described in this article.

References

- [1] M.I. Fernández, J.M. Oliva, X.L. Armesto, M. Canle L., J.A. Santalla, Extended planarity and π delocalization in triazine base-derivatives, *Chem. Phys. Lett.* 426 (2006) 290–295.
- [2] H.E. Birkett, J.C. Cherryman, A.M. Chippendale, P. Hazendonk, R.K. Harris, Molecular modelling studies of side-chain rotation in substituted triazine rings, *J. Mol. Struct.* 602–603 (2002) 59–70.
- [3] L.B. Favero, B. Velino, A. Maris, W. Caminati, The internal rotation and inversion pathways of the NH_2 group in equatorial amino cyclobutane, *J. Mol. Struct.* 612 (2002) 357–367.
- [4] K.B. Wiberg, C.M. Breneman, Resonance interactions in acyclic systems. 3. Formamide internal rotation revisited. Charge and energy redistribution along the C–N bond rotational pathway, *J. Am. Chem. Soc.* 114 (1992) 831–840.
- [5] A.N. Taha, N.S. True, Experimental ^1H NMR and computational studies of internal rotation of solvated formamide, *J. Phys. Chem. A* 104 (2000) 2985–2993.
- [6] I. Altarawneh, K. Altarawneh, A.H. Al-Muhtaseb, S. Alrawadi, M. Altarawneh, Theoretical study of thermochemical and structural parameters of chlorinated isomers of aniline, *Comput. Theor. Chem.* 985 (2012) 30–35.
- [7] M.R. Manaa, R.H. Gee, L.E. Fried, Internal rotation of amino and nitro groups in TATB: MP2 versus DFT (B3LYP), *J. Phys. Chem. A* 106 (2002) 8806–8810.
- [8] A.Y. Golovacheva, A.N. Romanov, V.B. Sulimov, Ab initio calculation of torsion and inversion barriers of the amino group in aminopyrimidines, *J. Phys. Chem. A* 109 (2005) 3244–3249.
- [9] D. Zeroka, James O. Jensen, Alan C. Samuels, Rotation/inversion study of the amino group in ethylamine, *J. Phys. Chem. A* 102 (1998) 6571–6579.
- [10] J.-M. Lehn, Conjecture: imines as unidirectional photodriven molecular motors—motional and constitutional dynamic devices, *Chem. Eur. J.* 12 (2006) 5910–5915.
- [11] T.R. Kelly, J.P. Sestelo, I. Tellitu, New molecular devices: in search of a molecular ratchet, *J. Org. Chem.* 63 (1998) 3655–3665.
- [12] M. Llunell, P. Alemany, J.M. Bofill, Conformational analysis of molecular machines: internal rotation and enantiomerization in triptycyl[3]helicene, *Chem. Phys. Chem.* 9 (2008) 1117–1119.
- [13] A. Shiroudi, M.S. Deleuze, S. Canneaux, Theoretical study of the oxidation mechanisms of naphthalene initiated by hydroxyl radicals: the OH-addition pathway, *J. Phys. Chem. A* 118 (2014) 4593–4610.
- [14] C.R. Crecca, A.E. Roitberg, Theoretical study of the isomerization mechanism of azobenzene and disubstituted azobenzene derivatives, *J. Phys. Chem. A* 110 (2006) 8188–8203.
- [15] J. Gálvez, A. Guirado, A theoretical study of topomerization of imine systems: inversion, rotation or mixed mechanisms?, *J. Comput. Chem.* 31 (2010) 520–531.
- [16] J. Wang, J. Gu, M.T. Nguyen, G. Springsteen, J. Leszczynski, From formamide to purine: an energetically viable mechanistic reaction pathway, *J. Phys. Chem. B* 117 (2013) 2314–2320.
- [17] M. Sánchez-Lozano, E.M. Cabaleiro-Lago, J.M. Hermida-Ramón, C.M. Estévez, A computational study of the protonation of simple amines in water clusters, *Phys. Chem. Chem. Phys.* 15 (2013) 18204–18216.
- [18] G. Kaur, Vikas, The mechanism of tautomerisation and geometric isomerisation in thioformic acid and its water complexes: exploring chemical pathways for water migration, *Phys. Chem. Chem. Phys.* 16 (2014) 24401–24416.
- [19] Spartan'10 Wavefunction, Inc. Irvine, CA.
- [20] B. Lucas, F. Grégorire, F. Lecomte, B. Reimann, J.P. Schermann, C. Desfrançois, Infrared spectroscopy of mass-selected neutral molecular systems without chromophore: the formamide monomer and dimer, *Mol. Phys.* 103 (2005) 1497–1503.
- [21] A.N. Taha, N.S. True, Pressure-dependent NMR spectroscopy indicates that internal rotation of gas-phase formamide follows statistical kinetics, *J. Phys. Chem. A* 104 (2000) 8609–8616.
- [22] A.N. Taha, S.M. Neugebauer Crawford, N.S. True, Determination of the internal rotation barrier of [^{15}N] formamide from gas-phase ^1H NMR spectra, *J. Am. Chem. Soc.* 120 (1998) 1934–1935.